Polyhedron 192 (2020) 114847

Contents lists available at ScienceDirect

Polyhedron

journal homepage: www.elsevier.com/locate/poly

Synthesis, structures, DNA-binding, cytotoxicity and molecular docking of $CuBr(PPh_3)$(diimine)

Bandar A. Babgi [a,*], Khlood H. Mashat [a], Magda H. Abdellattif [b], Muhammed N. Arshad [a,c], Khaled A. Alzahrani [a], Abdullah M. Asiri [a,c], Jun Du [d], Mark G. Humphrey [d], Mostafa A. Hussien [a,e]

[a] Department of Chemistry, Faculty of Science, King Abdulaziz University, P.O. Box 80203, Jeddah 21589, Saudi Arabia
[b] Department of Chemistry, Faculty of Science, Taif University, Al-Haweiah, P.O. Box 888, Taif 21974, Saudi Arabia
[c] Center of Excellence for Advanced Materials Research (CEAMR), King Abdulaziz University, P.O. Box 80203, Jeddah 21589, Saudi Arabia
[d] Research School of Chemistry, Australian National University, Canberra, ACT 2601, Australia
[e] Department of Chemistry, Faculty of Science, Port Said University, Port Said 42521, Egypt

ARTICLE INFO

Article history:
Received 17 July 2020
Accepted 12 October 2020
Available online 17 October 2020

Keywords:
Copper(I)
Phosphine
DNA-binding
Anticancer properties
Molecular docking

ABSTRACT

The copper(I) coordination compounds of general formula $[CuBr(PPh_3)(N\hat{}N)]$ (N^N = 2,2′-bipyridine (**1**), 1,10-phenanthroline (**2**), 4,4′-dimethyl-2,2′-bipyridine (**3**), 4,4′-dimethoxy-2,2′-bipyridine (**4**), 3-(2-pyridyl)-4,5-diphenyl-1,2,4-triazine (**5**), 4,7-diphenyl-1,10-phenanthroline (**6**), 5-nitro-1,10-phenanthroline (**7**), dipyrido[3,2-*a*:2′,3′-*c*]phenazine(**8**)) have been synthesized and characterized by elemental analysis, ^{31}P NMR spectroscopy and mass spectrometry. The structure of **5** and **7** were confirmed by X-ray crystallography. **5** is the second example to be reported with an unusual 4 *N*-triazine-ligated coordination mode of the 3-(2-pyridyl)-4,5-diphenyl-1,2,4-triazine. Calculated energies of the two possible bidentate modes of the ligand (2 *N*- and 4 *N*-triazine) at the copper center showed no significant difference, consistent with the absence of the steric hindrance at the metal center. Preliminary biological studies were conducted, highlighting the effect of the diimine ligands. **5** and **8** exhibited good cytotoxicity against prostate (PC-3), leukemia (MOLT-4) and breast (MCF-7) cancer cell lines, consistent with the presence of nitrogen heteroatoms and extended delocalized systems correlating with strong cytotoxic performance. Binding affinity studies against ct-DNA and docking studies with B-DNA and MDM2 protein highlighted the strong π interactions of **5** and **8**, with the planarity of the diimine ligand of the latter contributing to its better binding and cytotoxicity. The present results afford structural design requirements for new copper(I) coordination compounds with enhanced biological/physiochemical properties.

1. Introduction

Drug resistance and severe side-effects are well-known problems associated with platinum-based anticancer drugs [1,2] that have motivated extensive research in developing alternative metal-based therapeutic agents [3,4]. The cisplatin mechanism of action involves interference with DNA replication, interference with transcription, and modification of chromatin [5,6]. Therefore, development of new metal-based drugs is directed toward finding different metals and ligands that can non-covalently bind to DNA, aiming to reduce toxicity and enhance the therapeutic efficacy [7]. Among several modes of non-covalent binding, intercalation has received special interest in cancer therapy due to the potential to obstruct DNA replication and control the growth of cancer cells [8]. Polypyridyl ligands can bind to DNA in a non-covalent manner [9]. Hence, they are among the most used ligands in designing intercalating coordination compounds with promising anticancer properties [10].

In this context, copper polypyridyl coordination compounds have been of significant interest in DNA binding and cancer treatment, since copper ions play a key role in various biochemical processes [11]. Early work by Sadler and coworkers described the cytotoxic activities of copper(II) coordination compounds with salicylate and diimine ligands [12]. In a subsequent report, $[Cu(phen)(\text{L-threonine})(H_2O)]^+$ was shown to exhibit strong cytotoxic effects against human leukemia (HL-60) and human stomach cancer (SGC-7901) cell lines, DNA binding by intercalation being observed for this coordination compound [13]. A set of compounds of general formula $[Cu(O,N,N,O\text{-}HOCH_2CH_2NHCH_2CH_2N = CHC_6H_4O\text{-}2)(\text{diimine})]^+$ was assessed as potential anticancer agents, the IC_{50} values revealing that the example containing

* Corresponding author.
E-mail address: bbabgi@kau.edu.sa (B.A. Babgi).

https://doi.org/10.1016/j.poly.2020.114847
0277-5387/

3,4,7,8-tetramethyl-1,10-phenanthroline exhibits anticancer activity superior to cisplatin against human cervical epidermoid carcinoma cell line (ME180) [14]. A series of copper(II) polypyridyl compounds of general formula $[Cu(diimine)_2(H_2O)]^{2+}$ showed cytotoxicity towards several cancer cell lines, possibly through the formation of intracellular reactive oxygen species (ROS) and induction of apoptosis [15].

Recently, the interest in copper therapeutics has extended to the copper(I) polypyridyls. Copper(I) requires the use of soft ligands such as phosphines or carbenes to stabilize its coordination compounds by formation of strong metal-L bonds, exploiting the σ-donor and π-acceptor ability. Several copper(I) coordination compounds involving P-donor ligands have been reported to show significant cytotoxic activity. Coordination compounds of general formula $CuBr(PR_3)(phen)$ showed cytotoxic activity against a variety of cancer types including *cisplatin*-resistant phenotypes [16–18]. The effect of the phosphines on the anticancer, DNA binding, and physiochemical properties has been highlighted [16–18].

Motivated by our previous study with the anticancer-active $CuBr(PPh_3)(phen)$, our strategy in the current work is to assess the impact on DNA binding and anticancer activities of replacement of the phenanthroline with other polypyridyl ligands (potential DNA intercalating agents). In this paper, eight copper(I) compounds (Fig. 1) are reported, their interaction with DNA has been assessed spectroscopically, and their activity against four tumor cell lines has been evaluated. Docking studies have been undertaken to rationalize the DNA-binding and anticancer activities.

2. Experimental section

2.1. Chemicals and reagents

The HPLC grade solvents were used without further purification. 4,4′-Dimethyl-2,2′-bipyridine, 4,4′-dimethoxy-2,2′-bipyridine, 3-(2-pyridyl)-5,6-diphenyl-1,2,4-triazine, 4,7-diphenyl-1,10-phenanthroline, and 5-nitro-1,10-phenanthroline were obtained commercially and used as received. $CuBr(PPh_3)_3$ was prepared according to the literature [19] by stirring copper(II) bromide with ca. four molar equivalents of triphenylphosphine in refluxing ethanol under a nitrogen atmosphere. The product was obtained as a white precipitate after a few minutes. The known coordination compounds $CuBr(PPh_3)$(2,2′-bipyridine) (**1**) [20] and $CuBr(PPh_3)$(1,10-phenanthroline) (**2**) [21] were synthesized in accordance with established procedures. The dipyrido[3,2-*a*:2′,3′-*c*]phenazine (dppz) was prepared by the literature procedure [22] from the reaction of 1,10-phenanthroline-5,6-dione and *o*-phenylene diamine in refluxing ethanol.

2.2. Methods and instrumentation

Infrared spectra were recorded for powder samples of the compounds using a Bruker Alpha FT-IR; peaks are reported in cm^{-1}. ^{31}P NMR (242 MHz) spectra were recorded using a Bruker Avance 600 MHz spectrometer. The spectra are referenced to external H_3PO_4 (0.0 ppm, ^{31}P). High-resolution electrospray ionization (ESI) mass spectra were recorded using an Agilent Q-TOF 6520 instrument; all mass spectrometry data are reported as *m*/*z*. Absorption spectroscopy was performed using a MultiSpec-1501 UV–VIS spectrophotometer and 1 cm path-length quartz cells; bands are reported in the form: wavelength (nm).

2.3. Synthesis and characterization

2.3.1. General procedure for the synthesis of copper(I) compounds

Equimolar amounts of $CuBr(PPh_3)_3$ and the diimine ligand were stirred under nitrogen atmosphere in the appropriate amount of dichloromethane. The colorless solution turned yellow, orange or brown in a few minutes and was left stirring for 2 h. The reaction solution was then reduced in volume and 50 mL petroleum spirit (40–60 °C boiling point range) was added, leading to the precipitation of the product. The product was collected by filtration, washed with diethyl ether, and dried.

$CuBr(PPh_3)$(4,4′-dimethyl-2,2′-bipyridine) (3). 4,4′-Dimethyl-2,2′-bipyridine (0.118 g, 0.642 mmol) and $CuBr(PPh_3)_3$ (0.596 g, 0.642 mmol) were reacted to yield **3** as a yellow powder (0.258 g, 73%). HR ESI MS $[C_{30}H_{27}^{79}Br^{63}CuN_2P]^+$: calcd 588.0491, found 588.0471; $[C_{30}H_{27}^{81}Br^{63}CuN_2P]^+$: calcd 590.0491, found 590.0435. Anal. Calcd for $C_{30}H_{27}BrCuN_2P$: C, 61.07; H, 4.61; N, 4.75%; found: C, 60.23; H, 4.19; N, 4.26%. IR (solid): 522 cm^{-1} ν (P-Cu), 500 cm^{-1} ν(Cu–N). ^{31}P NMR δ: 31.5 (s, $P(C_6H_5)_3$).

$CuBr(PPh_3)$(4,4′-dimethoxy-2,2′-bipyridine) (4). 4,4′-Dimethoxy-2,2′-bipyridine (0.107 g, 0.494 mmol) and $CuBr(PPh_3)_3$ (0.460 g, 0.494 mmol) were reacted to yield **4** as a yellow powder (0.148 g, 48%). HR ESI MS $[C_{30}H_{27}^{79}Br^{63}CuN_2O_2P]^+$: calcd 620.0389, found 620.106; $[C_{30}H_{27}^{81}Br^{63}CuN_2O_2P]^+$: calcd 622.0369, found 622.0849. Anal. Calcd for $C_{30}H_{27}BrCuN_2O_2P$: C, 57.93; H, 4.38; N, 4.50%; found: C, 58.41; H, 4.71; N, 4.27%. IR (solid): 521 cm^{-1} ν (P-Cu), 489 cm^{-1} ν (Cu–N). ^{31}P NMR δ: 29.5 (s, $P(C_6H_5)_3$).

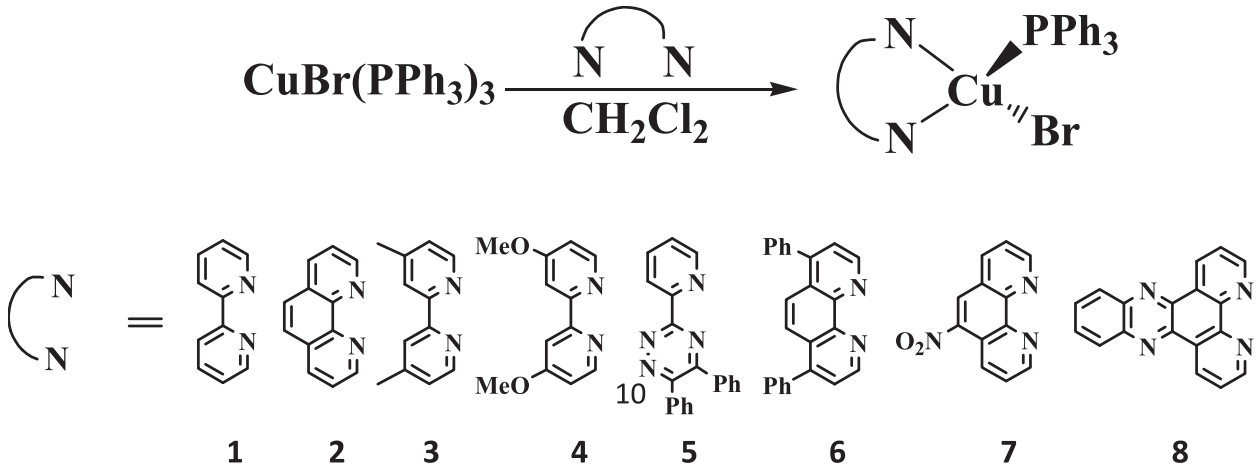

Fig. 1. Synthesis of coordination compounds **1** – **8**.

$CuBr(PPh_3)$(3-[2-pyridyl]-5,6-diphenyl-1,2,4-triazine) (5). $CuBr(PPh_3)_3$ (0.203 g, 0.218 mmol) and 3-(2-pyridyl)-5,6-diphenyl-1,2,4-triazine (0.071 g, 0.229 mmol) were reacted to yield **6** as a brown powder (0.127 g, 81%). HR ESI MS $[C_{38}H_{29}^{79}Br^{63}CuN_4P]^+$: calcd 712.0804, found 712.0910; $[C_{42}H_{31}^{81}Br^{63}CuN_4P]^+$: calcd 714.0784, found 714.0890. Anal. Calcd for $C_{38}H_{29}BrCuN_4P$: C, 63.74; H, 4.08; N, 7.82%; found: C, 63.98; H, 3.91; N, 7.46%. IR (solid): 525 cm^{-1} ν (P-Cu), 487 cm^{-1} ν(Cu–N). ^{31}P NMR δ: 30.4 (s, $P(C_6H_5)_3$).

$CuBr(PPh_3)$(4,7-diphenyl-1,10-phenanthroline) (6). 4,7-Diphenyl-1,10-phenanthroline (0.106 g, 0.319 mmol) and $CuBr(PPh_3)_3$ (0.296 g, 0.318 mmol) were reacted to yield **6** as an orange powder (0.202 g, 86%). HR ESI MS $[C_{42}H_{31}^{79}Br^{63}CuN_2P]^+$: calcd 736.0804, found 736.1240; $[C_{42}H_{31}^{81}Br^{63}CuN_2P]^+$: calcd 738.0708, found 738.1005. Anal. Calcd for $C_{42}H_{31}BrCuN_2P$: C, 68.34; H, 4.23; N, 3.80%; found: C, 68.09; H, 3.91; N, 3.36%. IR (solid): 522 cm^{-1} ν (P-Cu), 489 cm^{-1} ν (Cu–N). ^{31}P NMR δ: 30.2 (s, $P(C_6H_5)_3$).

$CuBr(PPh_3)$(5-nitro-1,10-phenanthroline) (7). 5-Nitro-1,10-phenanthroline (0.107 g, 0.475 mmol) and $CuBr(PPh_3)_3$ (0.439 g, 0.472 mmol) were reacted to yield **8** as a bright orange powder (0.274 g, 92%). HR ESI MS $[C_{30}H_{22}^{79}Br^{63}CuN_3O_2P]$: calcd 629.0029, found 629.0114; $[C_{30}H_{22}^{81}Br^{63}CuN_3O_2P]$: calcd 631.0009, found 631.0072. Anal. Calcd for $C_{30}H_{22}BrCuN_3O_2P$: C, 57.11; H, 3.51; N, 6.66%; found: C, 56.58; H, 3.28; N, 5.92%. IR (solid): 522 cm^{-1} ν (P-Cu), 501 cm^{-1} ν (Cu–N). ^{31}P NMR δ: 30.1 (s, $P(C_6H_5)_3$).

$CuBr(PPh_3)$(dppz) (8). Dipyrido[3,2-*a*:2′,3′-*c*]phenazine (0.104 g, 0.409 mmol) and $CuBr(PPh_3)_3$ (0.380 g, 0.409 mmol) were reacted to yield **9** as an orange powder (0.301 g, 84%). HR ESI MS $[C_{36}H_{25}^{79}Br^{63}CuN_4P]$: calcd 686.0396, found 686.0146; $[C_{36}H_{25}^{81}Br^{63}CuN_4P]$: calcd 688.0376, found 688.0137. Anal. Calcd for $C_{36}H_{25}BrCuN_4P$: C, 62.84; H, 3.66; N, 8.14%; found: C, 62.71; H, 3.48; N, 7.92%. IR (solid): 522 cm^{-1} ν (P-Cu), 496 cm^{-1} ν(Cu–N). ^{31}P NMR δ: 30.6 (s, $P(C_6H_5)_3$).

2.4. Crystallographic studies

Crystals of **5** and **7** suitable for analysis were obtained by vapor diffusion of hexane into solutions of the compounds in dichloromethane at 7 °C. Crystals were examined under a microscope and suitable samples were selected and mounted on an Agilent SuperNova (dual source) Agilent Technologies Diffractometer, equipped with microfocused Cu/Mo Kα radiation for data collection. The data collections were accomplished using CrysAlisPro software [23] at 296 K with Mo Kα radiation. The structure solutions were performed using SHELXS–97 [24] and refined by full–matrix least–squares methods on F^2 using SHELXL–97 [24], interfaced with WinGX [25]. All non–hydrogen atoms were refined anisotropically by full–matrix least-squares methods [24]. The figures were generated through PLATON [26] and ORTEP [27] interfaced with WinGX. All hydrogen atoms were positioned geometrically and treated as riding atoms with C—H = 0.93 Å and $U_{iso(H)} = 1.2U_{eq(C)}$ for all carbon atoms. For **7**, disorder corresponding to solvent could not been modelled satisfactorily, so was removed using Solvent Mask in Olex2. The crystal data were deposited at the Cambridge Crystallographic Data Centre with deposition numbers 1,892,006 (**5**) and 2,007,025 (**7** with solvent suppression using Solvent Mask). Crystal data can be obtained free of charge from CCDC, 12 Union Road, Cambridge CB21 EZ, UK (Fax: (+44) 1223 336–033; e-mail: data_request@ccdc.cam. ac.uk).

2.5. DNA binding studies

An aqueous solution of ct-DNA was prepared and the concentration was obtained from the absorbance values at 260 nm using the reported ε value of 6600 M^{-1} cm^{-1}, with the ratio of absorbances at 260 nm to that at 280 nm being 1.8 [28]. Spectroscopic investigations were carried out at pH 7.4 (using a phosphate buffer), keeping the molarity of the compounds at 20 μM while successively changing the concentration of ct-DNA. The photometric responses were followed after incubating the solutions for 2 min. From the absorbance values, the binding constants (K_b) of the compounds with ct-DNA were extracted from the Benesi-Hildebrand equation (Eq. (1)):

$$[A_o/(A - - A_o)] = [\varepsilon_g/(\varepsilon_{h-g} - \varepsilon_g)] + \{[\varepsilon_g/(\varepsilon_{h-g} - \varepsilon_g)] \times 1/(K_b[DNA])\} \quad (1)$$

$A_o/A - A_o$ (where A_o and A are the absorbance values of the compounds in the absence and presence of ct-DNA, respectively) was plotted against 1/[DNA] and the K_b values were calculated from the ratio of intercept to slope [29].

2.6. Anticancer studies

The cells were delivered by the Egyptian Holding Company for Biological Products and Vaccines (VACSERA), Giza, Egypt, and then reserved in the tissue culture unit. The cells were grown in RBMI-1640 medium, supplemented with 10% heat inactivated FBS, 50 units/mL of penicillin, and 50 mg/mL of streptomycin, and reserved in a humidified atmosphere containing 5% CO_2 [30,31]. The cells were maintained as monolayer cultures by serial sub-culturing. Cell culture reagents were sourced from Lonza (Basel, Switzerland). The anticancer activities of the compounds were evaluated against MCF-7 cells (breast cancer), HEPG-2 cells (liver cancer), PC-3 cells (prostate cancer), and MOLT-4 cells (leukemia cancer).

The sulforhodamine B (SRB) assay method was used to determine the cytotoxicity, as described by Skehan et al. [32]. Exponentially-growing cells were collected using 0.25% Trypsin-EDTA and seeded in 96-well plates at 1000-2000 cells/well in RBMI-1640 supplemented medium. After 24 h, cells were incubated for 72 h with various concentrations of the tested compounds. Following 72 h treatments, the cells were fixed with 10% trichloroacetic acid for 1 h at 4 °C. Wells were stained for 10 min at room temperature with 0.4% SRBC dissolved in 1% AcOH. The plates were air dried for 24 h and the dye was dissolved in Tris-HCl for 5 min with shaking at 1600 rpm. The optical density (OD) of each well was assessed spectrophotometrically at 564 nm with an ELISA microplate reader (ChroMate-4300, FL, USA). The measurements for each compound were undertaken three times. The IC_{50} values were calculated from a Boltzman sigmoidal concentration response curve using nonlinear regression fitting models (Graph Pad, Prism Version 5).

2.7. Molecular docking Studies:

Molecular docking studies were conducted with Molecular Operating Environment (MOE) 2008.10 (Chemical Computing Group Inc., Quebec, Canada, 2008). The docking scores were first attained utilizing the London dG scoring function in the MOE software, and were then improved using two unrelated refinement methods. Grid-Min pose and Force-field were employed to confirm that the refined poses of the coordination compounds were geometrically correct. Bond rotations were allowed, and the best five binding poses were then examined. To assess the binding free energy of the compounds toward DNA, the docking poses of the compounds and the co-crystallized structure of the B-DNA were docked (RSCP PDB code: 1BNA). RMSD values were used to assess the best binding pose. To evaluate the interaction between each compounds and MDM2 protein binding site, the docking poses of the compounds and the crystal structure of MDM2 bound to the transactivation domain of p53 (RSCP PDB code: 1YCR) were used for the docking calculation.

2.8. Computational Studies:

All quantum chemical calculations reported here used the GAUSSIAN 09 package [33]. Two methods were employed independently for the evaluation of the energy of $CuBr(PPh_3)$(3-[2-pyridyl]-5,6-diphenyl-1,2,4-triazine) (**5**) to compare the coordination compounds with *4 N*-triazine ligated and the *2 N*-triazine ligated. The density functional theory (DFT) [34] and second-order Møller-Plesset (MP2) perturbation [35] methods were used for geometry optimization and electronic structure determination. Our general protocol for DFT calculations employed the B3LYP [36] three-parameters hybrid functional and the Gen basis set [37], which consists of LANL2DZ [38] for Cu(I) and 6–311 + G(d, *p*) [39] for the other atoms. The dispersion-correction (D3) [40] function was also included in the DFT calculations and gave better structure results compared to the calculation without D3 correction. In regard to the MP2 calculations, the LANL2DZ basis set was employed to reduce the computational expense. All calculations were carried out in the gas phase and provided excellent results compared to the experimental data. Visualization of geometries, structure parameters, molecular orbitals, and vibrational modes were effected with GaussView 5 [41] software.

3. Results and discussion

3.1. Synthesis and characterization of the coordination compounds

The present study examines the effect of diimine ligand structural variation on the DNA-binding and anticancer activities of copper(I) compounds of general formula [Cu(N^N)(PPh_3)Br]. Tris (triphenylphosphine)copper(I) bromide is a key precursor for neutral copper-phosphine compounds; its importance as a building block arises from the bulkiness of the phosphine ligands, which cause considerable distortion in its tetrahedral geometry, leading to facile displacement of one or two of the phosphines. Stirring $CuBr(PPh_3)_3$ with the various diimine ligands in CH_2Cl_2 afforded **1**–**8**, the identities of which were confirmed by mass spectrometry, elemental analysis, and IR spectroscopy. ^{1}H NMR data of all compounds show only signals corresponding to PPh_3. The high dissociation rate of the phosphine ligand causes broadening of the diimine signals, to the extent that they are undetectable unless a small amount of free PPh_3 is added to the NMR tube. ^{31}P NMR spectra of **1**–**8** show singlet resonances for the ligated PPh_3 in the range 29–35 ppm Fig. S1. Further confirmation of the structures of **5** and **7** were provided by single-crystal X-ray diffraction studies (Fig. 3 and Fig. 4). Although the quality of the crystallographic data for **4** is poor, the studies were sufficient to confirm atomic connectivity; details are provided in the Supporting Information file (Figure S2).

Although the present study is directed toward the biological activities of the copper(I) compounds, the result of the reaction of the bulky diimine ligand 3-(2-pyridyl)-5,6-diphenyl-1,2,4-triazine with $CuBr(PPh_3)_3$ attracted our attention. The single-crystal diffraction study of the brown compound revealed an unusual coordination of the triazine ring to the copper atom. Recently reported coordination modes of the ligand at metal centers are summarized in Fig. 2. Coordination mode A is seen with the vast majority of reported coordination compounds, including those with Mn(II) [42], Ni(II) [43,44], Cu(I) [45], Cu(II) [46,47], Zn(II) [48,49], Ru(II) [50,51], Cd(II) [52], Sn(IV) [53], Re(I) [54], Re(III) [55], Re(V) [56], Pb(II) [57], and lanthanide [58,59] metal centers. Coordination mode C was reported for a dinuclear silver coordination compound of formula $[Ag_2(L)(NO_3)_2]$ [60]. There is only one example reported thus far with coordination mode B [46]. We presume that this is due to steric hindrance caused by the phenyl group at position 5. The current work has afforded the second example of coordination mode B.

To rationalize the unusual coordination mode (mode B), computational calculations were undertaken to evaluate the energies of the as-obtained mode B compound (**5**) and the unobserved mode A alternative. The two structures were optimized and the energies were evaluated using two methods (DFT-D3 and MP2: Table 1). The two methods suggest that the energies of both modes are almost the same (that of mode B is slightly less using both methods). The main finding from the calculated energies and geometries of the computed compounds (mode A and mode B) is that binding mode B does not afford a sterically congested structure.

In order to evaluate the accuracy of the data obtained by both methods, we compared selected bond lengths and angles obtained theoretically for mode B with that obtained from crystallography. MP2 afforded a better match with the experimental data, especially in predicting the bond angles (Table 2).

3.2. Crystallographic studies

Crystal and structure refinement data, hydrogen bonds, and bond lengths and angles for **5** and **7** are given in Tables S1–S12, respectively. The geometry around the Cu atom is trigonal pyramidal; the geometry indexes (τ_4) are 0.84 for **5** and 0.81 (molecule 1) and 0.83 (molecule 2) for **7** [18]. In **5**, the pyridyl and triazine rings are twisted out of coplanarity (dihedral angle: 12.691(9)°). The copper atom is ligated by two nitrogen atoms of the 3-pyridin-2-

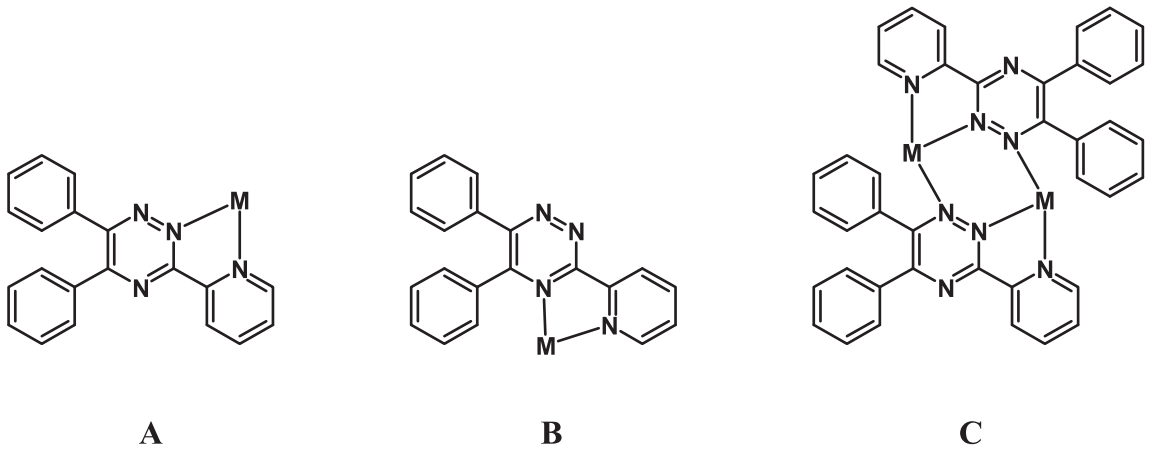

Fig. 2. Different coordination modes of 3-(2-pyridyl)-5,6-diphenyl-1,2,4-triazine.

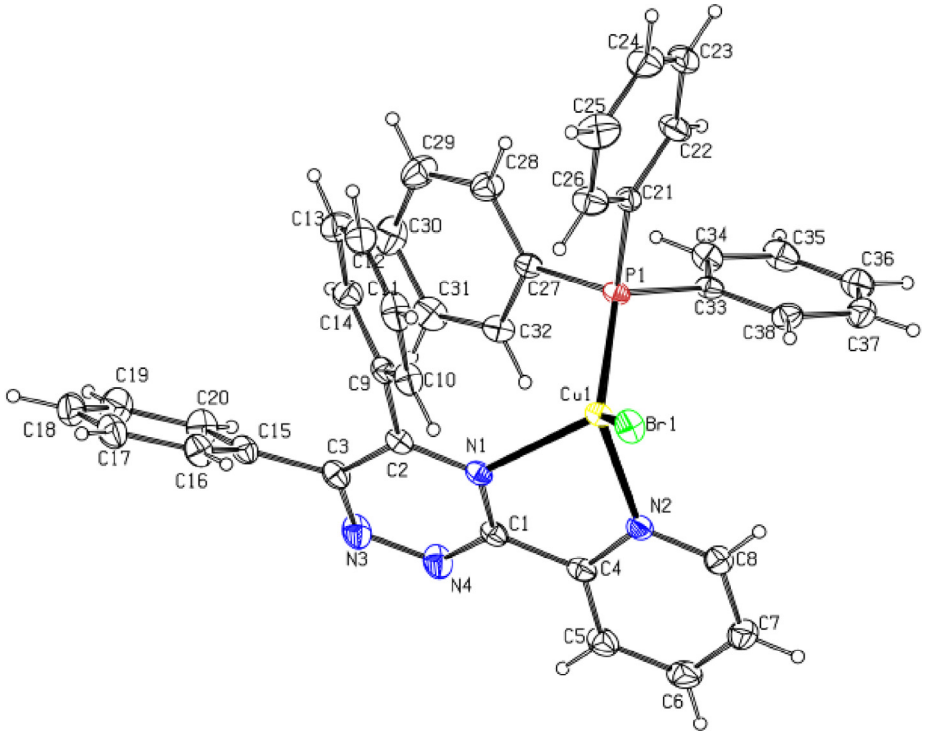

Fig. 3. *ORTEP* diagram for **5**; thermal ellipsoids are drawn at the 20% probability level.

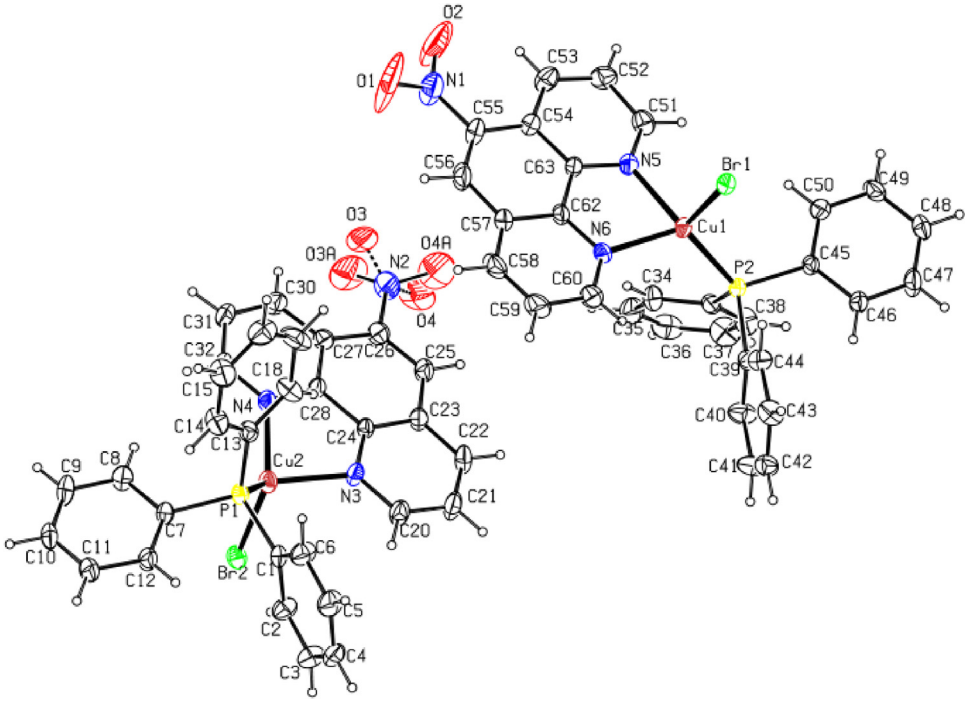

Fig. 4. *ORTEP* diagram for **7** showing the two independent molecules; thermal ellipsoids were drawn at the 20% probability level.

Table 1
Energies of optimized structures for binding modes A and B of the pyridyltriazine ligand with the $CuBr(PPh_3)$ fragment.

Computational method	Mode A model	Mode B model
MP2	−1891.4103 a.u	−1891.4210 a.u
DFT-D3	−4796.9070 a.u	−4796.9174 a.u

yl-[1,2,4]triazine, generating a five-membered ring motif (root-mean-square deviation: 0.1051(1) Å). The largest deviations from the plane (Cu1/N1/C1/C4/N2) are observed for N1 (-0.1433(1) Å) and C1 (0.1171(2) Å), while the puckering of this ring is described by parameters Q = 0.2418 Å, θ = 14.31(45)°, and φ = 17.59°. The two phenyl rings (C9-C14) and (C15-C20) attached to the triazine ring are twisted from its plane by 51.969(8)° and 49.439(7)°,

Table 2
Selected bond lengths and angles from crystallography and the corresponding data obtained using different theoretical methods.

Bond lengths/angles	Theoretical (MP2)	Theoretical (DFT-D3)	Experimental
Cu-P	2.325 Á	2.281 Á	2.1995(7) Á
Cu-Br	2.426 Á	2.406 Á	2.3842(4) Á
Cu-N_{py}	2.093 Á	2.145 Á	2.061(2) Á
Cu-$N_{triazine}$	2.166 Á	2.189 Á	2.1761(19) Á
Br-Cu-N_{py}	109.890^0	110.352^0	106.33(6)^0
Br-Cu-$N_{triazine}$	133.240^0	134.638^0	115.35(5)^0
Br-Cu-P	122.345^0	118.435^0	121.14(2)^0
P-Cu-N_{py}	111.247^0	110.261^0	119.69(6)^0
P-Cu-$N_{triazine}$	93.249^0	98.683^0	108.95(5)^0
N_{py}-Cu-$N_{triazine}$	78.682^0	76.354^0	77.66(8)^0

respectively. The most acute angle at copper is 77.66(8)° (N1-Cu-N2). Carbon atom C8 at (x,y,z) acts as a donor via H8 to the halogen atom Br1 at (-x,-y,-z) (Fig. S3), an interaction that generates dimers having a ten-membered ring motif that can be written as $R_2^2(10)$ [61] in mathematical notation. The molecules in the unit cell also participate in π... π interactions: the centroid–centroid distance is 3.975 Å and angle is 26.318° between the plane of (C33-C38) and the plane (N2/C4-C8), following the symmetry operation (-1/2 + x,1/2-y,+z) [62].

In **7**, there are two independent molecules in an asymmetric unit [Molecule I = C1-C32, Molecule II = C33-C63]. The N6-Cu1-Br1, N5-Cu1-Br1, N6-Cu1-*P*2, and N5-Cu1-*P*2 bond angles are 100.81(2), 108.79(17), 120.95(2) and 122.24(2), respectively, for molecule I, while the values are slightly different for molecule II [the N3-Cu2-Br2, N4-Cu2-Br2, N3-Cu2-*P*1, and N4-Cu2-*P*1 bond angles are 101.49(2)°, 107.30(16)°, 120.52(2)° and 1224.88(2)°, respectively]. The dihedral angles for the three phenyl rings around the P atoms are 82.07(3)°, 82.65(3)°, and 75.184(3)° for molecule I and 83.14(1)°, 82.88(3)°, and 75.91(3)° in molecule II. The 1,10 phenanthroline is twisted with dihedral angles of 83.77(3)°, 70.78(2)°, and 16.59(1)° for molecule I and 84.63(3)°, 66.71(2)°, and 18.24(2)° for molecule II. The availability of halogen and oxygen atoms gives rise to formation of hydrogen bonding interactions. The bromo (Br1), as acceptor atom, is connected to the C25, as donor atom, via H25. Similarly, bromo (Br2) is connected to the C56 through H56. The oxygen atom O4a is connected to hydrogen atoms of two adjacent carbon atoms (C51 and C52), generating five-membered rings that can be presented as $R_2^1(5)$ [61] Figs. S4–S6. These interactions generate a two-dimensional network across the *ac* plane.

In comparison with **5**, the Cu-Br bond length in **7** is longer [2.4337(12) Á & 2.4400 cf. 2.4183(9) Á]. Although there are two independent molecules in the unit cell, there are no π ... π interactions between the planes of the aromatic groups in the molecules.

3.3. DNA-binding studies

The electronic absorption spectra of the copper(I) compounds were collected in dimethyl sulfoxide (DMSO) solutions at room temperature, the absorption maxima data being presented in Table 3. The electronic spectra of **1**–**8** display intense absorption bands around 265–295 nm corresponding to π → π* transitions. In addition, broad low-intensity bands are observed in the range 340 to 410 nm for **1**–**4**, in the range 360 to 450 nm for **6**, and in the range 360 to 500 nm for **5**, **7**, and **8**. These broad bands are assigned as metal-to-ligand charge transfer (MLCT) in character [63].

Table 3
UV–vis spectroscopic data and binding constants (K_b) for 1–8

Compound	Absorption Maxima [λ_{max} (nm)]	Binding Constant [K_b (M^{-1}) × 10^5]
1	278, br sh 349	6.7
2	272, br sh 373	1.4
3	287, br sh 342	5.0
4	265, br sh 322	5.0
5	285, br sh 401	14.0
6	289, br sh 360	10.0
7	272, br sh 368	10.0
8	273, br sh 400	20.0

*br sh (broad shoulder)

Metal compounds can bind to DNA via different modes of interaction, including minor groove binding, major groove binding, intercalation interactions, and electrostatic interactions [64]. UV–vis absorption spectroscopy can be used as an effective tool to study the general interactions between metal compounds and DNA, by following the changes in the absorption of the DNA or the compound [65] Fig. S7. The absorption spectra of the compounds were measured while gradually increasing the concentrations of DNA in solutions containing a constant concentration of the compounds. The compounds show reductions in molar absorptivity of the π → π* absorption band (hypochromic shifts), indicating binding of the compounds to DNA. The calculated K_b values of **1** – **8** are listed in Table 3, the data indicating that there are significant variations in K_b values, consistent with a strong influence of the diimine ligands. In general, the more extended the π-delocalized system, the greater the binding affinity toward ct-DNA. **8** has the largest K_b value due to the planar and highly delocalized dipyrido[3,2-*a*:2′,3′-*c*]phenazine ligand; compounds of this ligand with some metal centers are known to intercalate with DNA [66,67].

3.4. Anticancer activity

1–**8** were examined against four cancer cell lines, the cytotoxicity of the compounds being listed in Table 4. From the obtained data, our compounds show good anticancer activity against the prostate (PC-3) cancer cell line. More specifically, **4**, **5**, **6** and **8** show the best cytotoxicity against PC-3, due possibly to their more electron rich and highly extended delocalized systems. Only **5** and **8**, with the largest number of nitrogen heteroatoms, exhibit good cytotoxicity against the leukemia (MOLT-4) and breast (MCF-7) cancer cell lines. None of the compounds display strong activity against the liver cancer cell line. In summary, **5** and **8** have good anticancer potential against several cell lines.

Table 4
Cytotoxicity of Cu(I) compounds in DMSO solutions.

Compound	IC_{50} (μM) ± SD			
	MCF-7 (breast cancer)	HEPG-2 (liver cancer)	PC-3 (prostate cancer)	MOLT-4 (leukemia cancer)
1	108.66 ± 0.06	69.46 ± 0.04	49.03 ± 0.03	47. 41 ± 0.50
2	25.00 ± 0.04	66.04 ± 0.06	33.18 ± 0.01	88.06 ± 0.01
3	57.10 ± 0.05	106.33 ± 0.09	69.70 ± 0.03	96.28 ± 0.08
4	57.24 ± 0.07	90.70 ± 0.07	23.04 ± 0.03	79.43 ± 0.00
5	26.67 ± 0.00	51.31 ± 0.02	26.67 ± 0.00	27.19 ± 0.02
6	55.97 ± 0.02	66.44 ± 0.00	23.61 ± 0. 03	54.29 ± 0.12
7	106.15 ± 0.05	66.28 ± 0.01	37.12 ± 0.05	59.60 ± 0.21
8	21.38 ± 0.00	47.47 ± 0.02	21.38 ± 0.00	31.03 ± 0.05
Cisplatin	16.00 ± 0.06	–	39.99 ± 0.05	–

3.5. Molecular docking studies

The most common mechanisms identified for copper(I) compounds similar to our current compounds are (**1**) interactions with DNA [68] and (2) the induction of cellular apoptosis [17,69,70]. Molecular docking studies were conducted to obtain insight into the contribution of the diimine ligands in the DNA-binding and the p53-MDM2 binding inhibition. The compounds were constrained to possess tetrahedral geometries while maintaining diimine planarity, in order to avoid unlikely distortions. The compounds were computationally docked with all the possible sites on the B-DNA to aid in rationalizing the trends from the binding constant values, the data obtained being collected in Table S9. **5**, **6** and **8** scored the highest binding affinities according to the docking results (Table S9); all three have extended π -delocalized diimine ligands that are capable of establishing π interactions. Among these three compounds, **8** has the best binding affinity value, which can be rationalized from the planarity of the ligand and the extended delocalization allowing formation of several H-π interactions (Fig. 5).

We also explored docking our compounds with MDM2, which is an important inhibiting protein that binds to the p53 tumor suppressor. The dissociation of MDM2 from p53 causes the activation of p53, inducing a cell cycle arrest which leads to apoptosis. The inactivation of MDM2 by its strong binding with compounds may therefore induce apoptosis [71]. In the present studies, MCL0527 was employed as a benchmark because it is a known inhibitor of p53-MDM2 interactions [71]. Compared to MCL0527, all eight copper compounds have better binding scores to MDM2. The presence of the highly delocalized planar systems improves the binding capabilities through various π interactions (Table S13). In particular, **8** has the ability to establish strong interactions with MDM2 via the planar dppz ligand (Fig. 5).

4. Conclusion

Copper(I) compounds with a diimine-phosphine ligand set have been synthesized and characterized by elemental analysis, ^{31}P NMR spectroscopy, and mass spectrometry. Confirmation of the

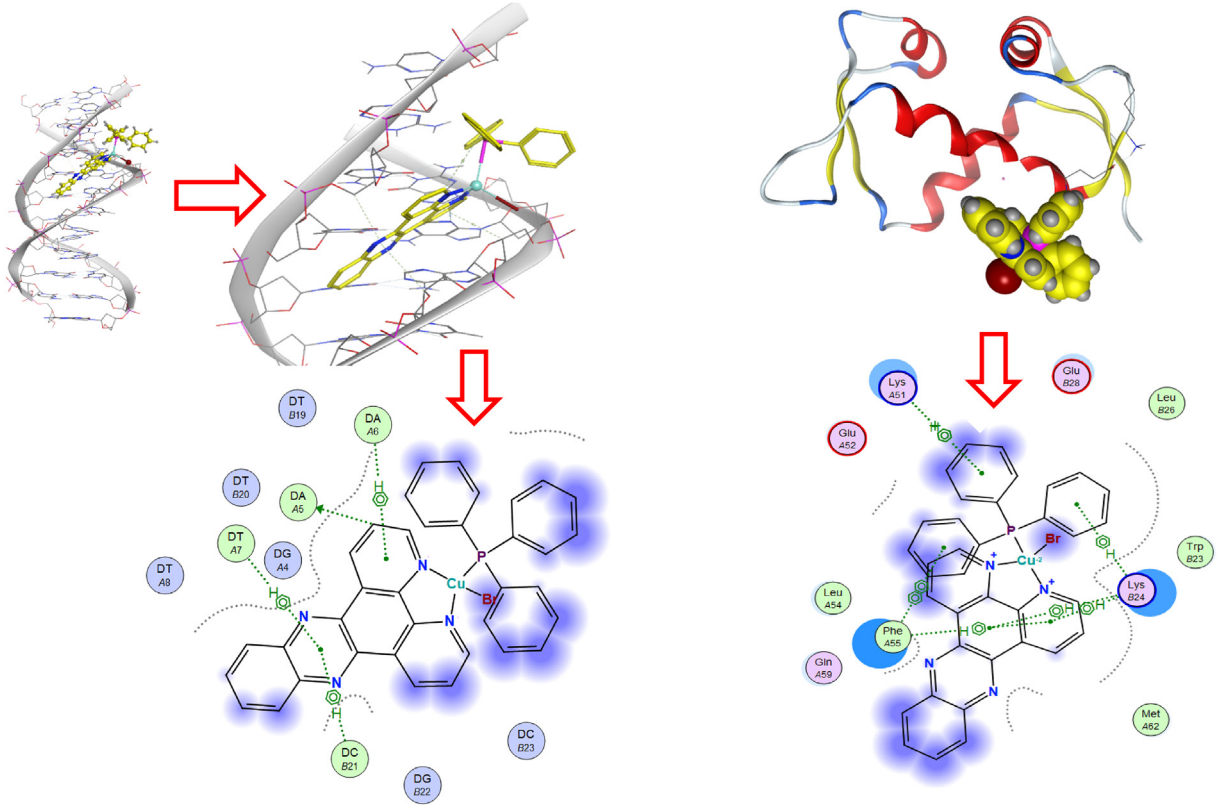

Fig. 5. 3D and 2D views of interactions of **8** with B-DNA (left) and MDM2 (right) as calculated by MOE.

structures of **5** and **7** was provided by X-ray crystallography, the study of **5** revealing the second example of an unusual bonding mode (*4 N*-triazine ligated) of the bidentate ligand 3-(2-pyridyl)-4,5-diphenyl-1,2,4-triazine. Computational studies indicated no significant difference in the energies of the obtained compound (mode B) and the alternative isomer (mode A), consistent with an absence of steric hindrance at the metal center of **5**. Preliminary biological studies were conducted aiming to assess the effect of the diimine ligands. All the studied compounds showed good cytotoxicity against the prostate (PC-3) cancer cell line. However, only **5** and **8** exhibited good cytotoxicity against leukemia (MOLT-4) and breast (MCF-7) cancer cell lines. In these cases, the additional nitrogen heteroatoms and more extended π -systems are proposed to be key factors inducing the enhanced anticancer activities. DNA-binding and docking studies with intracellular targets highlighted the ability of the compounds with highly delocalized diimine ligands to exploit stronger π interactions and achieve stronger binding; the planarity is an important feature here, resulting in better targeting and better cytotoxicity in **8**. Overall, the current results afford structural indicators for the design of derivatives with improved biological profiles.

Author contributions

BAB conceived of the presented idea. BAB and KHM synthesized and characterized the compounds. MHA investigated the anti-cancer properties. MNA, AMA and JD did the XRD measurements and write the structures description. KAA performed the computational studies. MAH and KHM run the DNA-binding studies. MAH and MHA did the molecular docking studies. BAB supervised the findings of this work. BAB and MGH discussed the results and contributed to the final manuscript.

Declaration of Competing Interest

The authors declare that they have no known competing financial interests or personal relationships that could have appeared to influence the work reported in this paper.

Acknowledgments

This project was funded by the Deanship of Scientific Research (DSR), King Abdulaziz University, Jeddah, Saudi Arabia under grant no. (KEP-44-130-40). The authors, therefore, acknowledge with thanks DSR technical and financial support.

Appendix A. Supplementary data

Supplementary data to this article can be found online at https://doi.org/10.1016/j.poly.2020.114847.

References

[1] S. Dasari, P.B. Tchounwou, Eur. J. Pharmacol. 740 (2014) 364–378.
[2] P. Heffeter, U. Jungwirth, M. Jakupec, C. Hartinger, M. Galanski, L. Elbling, M. Micksche, B. Keppler, W. Berger, Drug Resist. Updates 11 (2008) 1–16.
[3] M. Zaki, F. Arjmand, S. Tabassum, Inorg. Chim. Acta 444 (2016) 1–22.
[4] M. Yang, U. Bierbach, Eur. J. Inorg. Chem. 12 (2017) 1561–1572.
[5] E. Wong, C.M. Giandomenico, Chem. Rev. 99 (1999) 2451–2466.
[6] X.Y. Wang, Z.J. Guo, Dalton Trans. 12 (2008) 1521–1532.
[7] M.J. Clarke, F. Zhu, R.F. Dominic, Chem. Rev. 99 (1999) 2511–2533.
[8] H.-K. Liu, P.J. Sadler, Acc. Chem. Res. 44 (2011) 349–359.
[9] T. Phillips, I. Haq, A.J.H.M. Meijer, H. Adams, I. Soutar, L. Swanson, M.J. Sykes, J. A. Thomas, Biochemistry 43 (2004) 13657–13665.
[10] S. Thota, D.A. Rodrigues, D.C. Crans, E.J. Barreiro, J. Med. Chem. 61 (2018) 5805–5821.
[11] C. Santini, M. Pellei, V. Gandin, M. Porchio, F. Tisato, C. Marzano, Chem. Rev. 114 (2014) 815–862.
[12] J.D. Ranford, P.J. Sadler, D.A. Tocher, Dalton Trans. (1993) 3393–3399.
[13] S. Zhang, Y. Zhu, C. Tu, H. Wei, Z. Yang, L. Lin, J. Ding, J. Zhang, Z. Guo, J. Inorg. Biochem. 98 (2004) 2099–2106.
[14] V. Rajendiran, R. Karthik, M. Palaniandavar, H. Stoeckli-Evans, V.S. Periasamy, M.A. Akbarsha, B.S. Srinag, H. Krishnamurthy, Inorg. Chem. 46 (2007) 8208–8221.
[15] P. Nagababu, A.K. Barui, T. Bathini, S. Gampa, S. Satyanarayana, C. Patra, B. Sreedhar, J. Med. Chem. 58 (2015) 5226–5241.
[16] C. Marzano, M. Pellei, D. Colavito, S. Alidori, G.G. Lobbia, V. Gandin, F. Tisato, C. Santini, J. Med. Chem. 49 (2006) 7317–7324.
[17] V. Gandin, M. Porchia, F. Tisato, A. Zanella, E. Severin, A. Dolmella, C. Marzano, J. Med. Chem. 56 (2013) 7416–7430.
[18] K.H. Mashat, B.A. Babgi, M.A. Hussien, M.N. Arshad, M.H. Abdellatif, Polyhedron 158 (2019) 164–172.
[19] R. Gujadhur, D. Venkataraman, J.T. Kintigh, Tetrahedron Lett. 42 (2001) 4791–4793.
[20] F.H. Jardine, L. Rule, A.G. Vohira, J. Chem. Soc. A (1970) 238–240.
[21] D.V. Allen, D. Venkataraman, J. Org. Chem. 68 (2003) 4590–4593.
[22] J.E. Dickeson, L.A. Summers, Aust. J. Chem. 23 (1970) 1023–1027.
[23] Agilent, CrysAlis PRO, Agilent Technologies, Yarnton, England, 2012.
[24] G.M. Sheldrick, Acta Crystallogr. C 71 (2015) 3–8.
[25] L.J. Farrugia, J. Appl. Crystallogr. 32 (1999) 837–838.
[26] A.L. Spek, PLATON – A Multipurpose Crystallographic Tool, Utrecht University, Utrecht, 2005.
[27] L.J. Farrugia, J. Appl. Crystallogr. 45 (2012) 849–854.
[28] L. Tabrizi, H. Chiniforoshan, New J. Chem. 41 (2017) 10972–10984.
[29] A. Wolfe, G.H. Shimer, T. Meehan, Biochem. 26 (1987) 6392–6396.
[30] D. Muanza, B. Kim, K. Euler, L. Williams, Pharm. Biol. 32 (1994) 337–345.
[31] J. Pezzuto, C. Che, D. McPherson, P. Zhu, G. Topcu, C. Erdelmeier, G. Cordell, J. Nat. Prod. 54 (1991) 1522–1597.
[32] P. Skehan, R. Storeng, D. Scudiero, A. Monks, J. McMahon, D. Vistica, J.T. Warren, H. Bokesch, S. Kenney, M.R.J. Boyd, Nat. Cancer Inst. 82 (1990) 1107–1112.
[33] P. Hohenberg, W. Kohn, Phys. Rev. 136 (1964) B864–B871.
[34] C. Møller, M.S. Plesset, Phys. Rev. 46 (1934) 618–622.
[35] A.D. Becke, J. Chem. Phys. 98 (1993) 5648–5652.
[36] C. Lee, W. Yang, R.G. Parr, Phys. Rev. B 37 (1988) 785–789.
[37] P.J. Hay, W.R. Wadt, J. Chem. Phys. 82 (1985) 270–283.
[38] P.J. Hay, W.R. Wadt, J. Chem. Phys. 82 (1985) 299–310.
[39] K. Raghavachari, G.W. Trucks, J. Chem. Phys. 92 (1989) 1062–1065.
[40] S. Grimme, J. Antony, S. Ehrlich, S. Krieg, J. Chem. Phys. 132 (2010) 154104.
[41] GaussView 5.0, (Gaussian Inc., Wallingford, CT, USA) 2009.
[42] N.E. Eltayeb, T.S. Guan, B.M. Yamin, Acta Crystallogr. E 62 (2006) m2284–m2286.
[43] M.C. Aragoni, M. Acra, S.L. Coles, F.A. Devillanova, M.B. Hursthouse, F. Isaia, V. Lippolis, Dalton Trans. 41 (2012) 6611–6613.
[44] J.G. Malecki, B. Machura, A. Switlicka, Struct. Chem. 22 (2011) 77–87.
[45] J. Lopes, D. Alves, T.S. Morais, P.J. Costa, M.F.M. Piedade, F. Marques, M.J. Villa de Brito, G.M. Helena, J. Inorg. Biochem. 169 (2017) 68–78.
[46] A. Yamada, T. Mabe, R. Yamane, K. Noda, Y. Wasada, M. Inamo, K. Ishihara, T. Suzuki, H.D. Takagi, Dalton Trans. 44 (2015) 13979–13990.
[47] B. Machura, A. Switlicka, R. Kruszynski, J. Mrozinski, J. Klak, J. Kusz, Polyhedron 27 (2008) 2959–2967.
[48] F. Marandi, A.A. Soudi, A. Morsali, R. Kempe, Z. Anorg. Allg. Chem. 631 (2005) 3070–3073.
[49] F. Marandi, H.-K. Fun, S. Chantrapromma, J. Coord. Chem. 62 (2009) 2155–2163.
[50] B. Therrien, C. Said-Mohamed, G. Suess-Fink, Inorg. Chim. Acta 361 (2008) 2601–2608.
[51] S. Maji, C. Chatterjee, S.M. Mobin, G.K. Lahiri, Eur. J. Inorg. Chem. 21 (2007) 3425–3434.
[52] A.A. Soudi, A. Ramazani, F. Marandi, A. Morsali, J. Coord. Chem. 60 (2007) 1427–1433.
[53] C.L. Tan, K.M. Lo, S.W. Ng, Acta Crysta. E 65 (2009) m694.
[54] S. Das, B.K. Panda, Polyhedron 25 (2006) 2289–2294.
[55] B. Machura, M. Wolff, A. Switlicka, R. Kruszynski, J. Morzinski, Struct. Chem. 21 (2010) 761–769.
[56] S. Das, A. Chakravorty, Eur. J. Inorg. Chem. 11 (2006) 2285–2291.
[57] F. Marandi, H.-K. Fun, Q.C. Kheng, J. Coord. Chem. 63 (2010) 2113–2121.
[58] L. Panayiotidou, M. Stylianou, N. Arabatzis, C. Drouza, P. Lianos, E. Stathatos, A. D. Keramidas, Polyhedron 52 (2013) 856–865.
[59] G.L. Guillet, I.F.D. Hyatt, P.C. Hillesheim, K.A. Abboud, M.J. Scott, New J. Chem. 37 (2013) 119–131.
[60] F. Marandi, N. Hosseini, H. Krautscheid, D. Laessig, J. Lincke, M. Rafiee, Y.A. Asl, J. Mol. Struct. 1006 (2011) 324–329.
[61] J. Bernstein, R.E. Davis, L. Shimoni, N.-L. Chang, Angew. Chem. Int. Ed. 34 (1995) 1555–1575.
[62] R. Kruszynski, T. Sieranski, Cryst. Growth Des. 16 (2016) 587–595.
[63] D. Chen, W.-X. Chai, L. Song, Trans. Metal. Chem. 43 (2018) 517–527.
[64] H. Ihmels, D. Otto, Top. Curr. Chem. 258 (2005) 161–204.
[65] B.J. Pages, D.L. Ang, E.P. Wright, J.R. Aldrich-Wright, Dalton Trans. 44 (2015) 3505–3526.
[66] X. Li, A.K. Gorle, M.K. Sundaraneedi, F.R. Keene, J.G. Collins, Coord. Chem. Rev. 375 (2018) 134–147.
[67] K. Palanichamy, A.C. Ontko, Inorg. Chim. Acta 359 (2006) 44–52.
[68] Colina-Vegas, L.; Villarreal, W.; Navarro, M.; Ch 5: Copper(I)–phosphine complexes: a promising approach in the search for antitumor agents;

Copper(I) Chemistry of Phosphines, Functionalized Phosphines and Phosphorus Heterocycles, Balakrishna, M. S. (Ed), Elsevier, 2019, 109–143.
[69] Marzano, C.; Tisato, F.; Porchia, M.; Pellei, M.; Gandin, V.; Ch 3: Phosphine copper(I) complexes as anticancer agents: biological characterization. Part II.; Copper(I) Chemistry of Phosphines, Functionalized Phosphines and Phosphorus Heterocycles, Balakrishna, M. S. (Ed), Elsevier, 2019, 83-107.
[70] U.K. Komarnicka, S. Kozieł, P. Zabierowski, R. Kruszyński, M.K. Lesiów, F. Tisato, M. Porchia, A. Kyzioł, J. Inorg. Biochem. 203 (2020) 110926.
[71] W. Wang, S. Shangguan, N. Qiu, C. Hu, L. Zhang, Y. Hu, Bioorg. Med. Chem. 21 (2013) 2879–2885.